117 Numerical Simulation of DI Diesel Engine's Combustion Chamber Using Several Turbulence Models During Intake and Compression Strokes

(1),(2) (1) (1)
Seyed Ali Jazayeri, Masoud Mirzaei, Javad Kheyrollahi

(1) (2)
KN Toosi University of Technology /University of Victoria

This paper presents a CFD approach simulation of flow field during intake and compression of a four strokes IC engine. In this model a dynamic mesh is used to simulate the moving boundaries of engine parts, such as piston and valves. Computational domain, which is a precise model of one cylinder, is meshed to 300,000-500,000 cells. In our solution three different two-equation turbulence models are used. The capability of each model is highlighted and the results are compared with relevant works.

The focus of these turbulence models and three-dimensional simulation of engine flow are to validate the reliability of flow characteristics. The results accurately demonstrate the three-dimensional characteristics of air motion in the swirl chamber and development of vortices.

***Keywords*: Automotive General, Engine, Computer Application / Flow Field, Dynamic Mesh, Turbulence**

1. INTRODUCTION

In recent years, great amount of work has been carried out to improve diesel engines efficiency and emission standards. This has been a continuing trend due to governmental legislations and laws, especially in the area of land transportation. The fuel injection system is an engine sub-system, which has the largest potential to meet this requirement through controlling the combustion process that is highly influenced by efficient air-fuel mixture, particularly in high-speed direct injection Diesel engines, which are employed for land transportation.

In high-speed direct injection Diesel engines, flow conditions during the induction process and its evolution during compression stroke near top dead center are critical for combustion process improvement [1].

Steady state experimental tests are used to characterize the flow motion generated by the induction system [2] and Yun [3] considered further parameters to evaluate the bulk motion of air in cylinder. Experimental results help to get a better insight in to flow variables inside the cylinder.

Other experimental techniques are to measure the velocity field in the steady flow test using laser Doppler velocimetry (LDV) [4]. This method provides accurate results and more information about flow field, but is costly and time consuming. The LDV technique should used while the engine is working and complex experimental setup with good optical access to combustion chamber is necessary [5].

Another approach is application of three dimensional calculation codes, which solves the governing equations, and gives detailed descriptions of the mean velocity and the turbulent velocity fields. In diesel engines, the CFD models have to take care of specific problems linked to the flow unsteadiness, high Reynolds numbers involved, and the complex variable geometry of the solid boundaries.

The speed and extent to which the fuel spray penetrates across the combustion chamber are strongly dependent on gas/liquid density ratio and has an important influence on air utilization and fuel air mixing rate. Spray penetration depends on pressure, temperature and the swirl ratio of the gas in the combustion chamber. Spray tip penetration varies with time and swirl rate. Initial average drop diameter is proportional to the gas density and relative velocity between the liquid and gas (taken as the mean injection velocity). The spreading vapor region of the spray is carried around the chamber by the swirling airflow [6].

In this work, an extensive study of the flow characteristics inside the cylinder of a heavy-duty direct-injection Diesel engine (OM355, locally manufactured engine) is carried out using different CFD models. The flow calculations is carried out during the intake and compression strokes for original piston bowl and combustion chamber geometries, taking into account valve movement and ports without any simplification later validation is shown though comparing results with other works.

2. CASE DESCRIBTION

The reference is a single-cylinder of a six-cylinder direct-injection engine (Table 1) with two separate intake ports which their outlets through inlet valves are tangential to the cylinder wall, also has a twin exhaust ports which are meshed together, this model and cylindrical bowl configuration in piston are shown in Fig. 1.

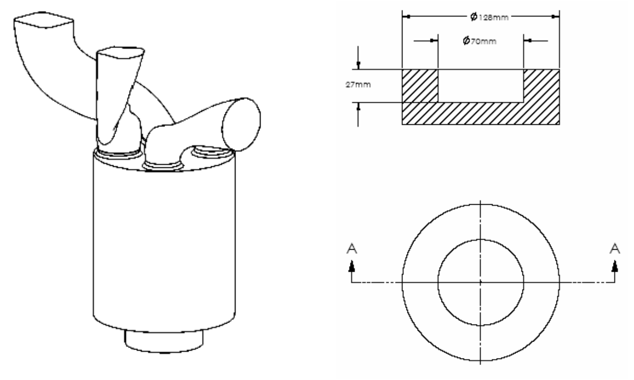

Fig. 1: Single-cylinder of the engine and detailed piston crown.

Table 1.Engine Specification (OM355)

Bore	128.0 mm
Stroke	150.0 mm
Connecting rod length	280.0 mm
Displacement	1930.2 cm3
Intake valve diameter	42.0 mm
Exhaust valve diameter	38.0 mm
Intake valve opening	31 BTDC
Intake valve closing	60 ABDC
Exhaust valve opening	62 BBDC
Exhaust valve closing	25 ATDC

Engine cylinder calculation is based on real intake and compression strokes operating condition of the motored engine simulation at 1000 rpm. Two different initial conditions can be used for simulation [7], either from exhaust stroke or from intake stroke. The second case is considered because in the other case the run time will increase, computational domain will be larger and simulation will be extended by 180 crank angles. Initial values of pressure and temperature are chosen from experimental data. Fig. 2 shows the computational domain which is used for calculations.

3. NUMERICAL METHODOLOGY

Discretized Navier–Stokes equations are solved using Fluent 6.1.18 Segregated solver. Three turbulence models including standard $\kappa-\varepsilon$, RNG $\kappa-\varepsilon$ and SST $\kappa-\omega$ turbulence models for high Reynolds numbers with wall function are used.

The program uses PISO pressure-correction algorithm and the first order upwind differencing scheme is used for the momentum, energy and turbulence equations. The calculations start at the beginning of intake stroke, proceeds during the intake and compression stroke and finish 10 degrees after the end of compression stroke. This is because the injection starts at about 15 degrees before TDC and there is a delay of 9 degrees between the start of injection and the start of combustion [6]. After this stage, the combustion process mainly influences the flow characteristics.

The initial values for pressure and temperature were obtained from experimental tests, and these parameters are assumed homogenous for the whole domain. The engine intake process governs many important aspect of the flow within the cylinder and this can eliminate the effect of initial conditions [6] so in this research, the residual swirl flow in cylinder at the end of exhaust stroke was not taken into account and flow is taken as quiescent initially. Constant pressure boundary conditions were assigned at both inlets by neglecting the dynamic effects of the manifold. Lateral walls of the valves and ports were considered adiabatic so constant temperature boundary conditions were assigned separately for the head, the cylinder wall and the piston crown.

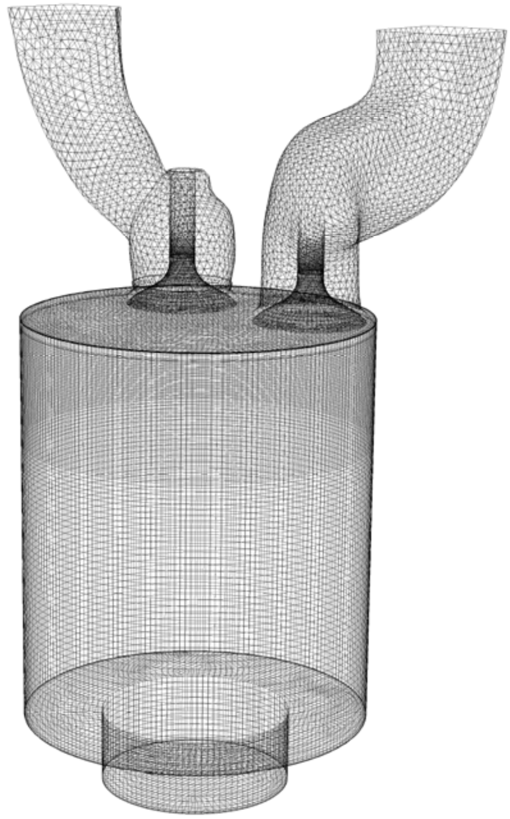

Fig. 2: Computational domain used for calculations.

4. GRID INDEPENDENCE STUDY

Computational domain cells for confined cylinder vary from 146,800 cells at top dead center, to 525,150 cells at bottom dead center. GAMBIT 2.0.0 is used for grid generation.

Hexahedral cells are used for combustion chamber, piston bowl and valve zones and tetrahedral cells are used in intake zones because of complicated geometry. Hexahedral cells have been preferred for the grid generation since they provide better accuracy and stability than tetrahedral cells [13]. Because of its complex geometry and moving boundaries, the computational domain is divided into thirty separate zones, which are late linked together. Fig. 3 shows this domain at valve section.

The grid generation method used is capable of modeling the dynamic movement of boundaries. During the compression stroke, once the intake valves are closed, the boundary

Table 2. Three different mesh cases are shown in this table.

Cases	Number of cells at BDC	Cell dimension at combustion chamber (mm)	Cell dimension at valve domain (mm)	Run time for eight iterations in each time step (minute)
Case 1	525,150	2	1	One
Case 2	1,280,500	1	0.5-0.75	Four
Case 3	2,740,500	0.75	0.5	Six

conditions of valve inlet walls are changed. In order to ensure grid independence and improve the accuracy of the results, three sets of calculations during intake stroke are carried out using different grid sizes, then at these calculated domains the velocity magnitudes are compared at a line located 4 mm from cylinder head where the turbulence intensity gradient is maximum because of valve opening. (Fig. 4)

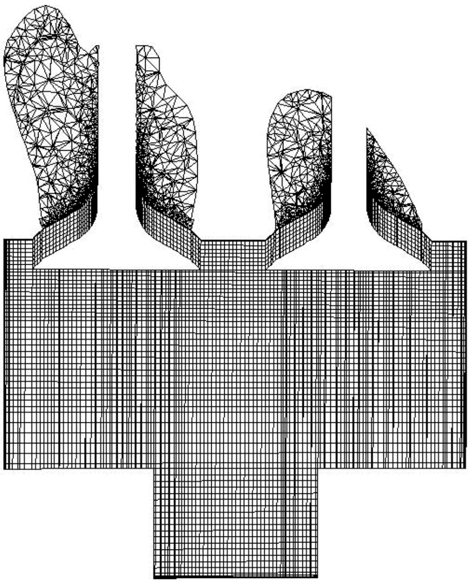

Fig. 3: Computational domain at intake valves on section CC.

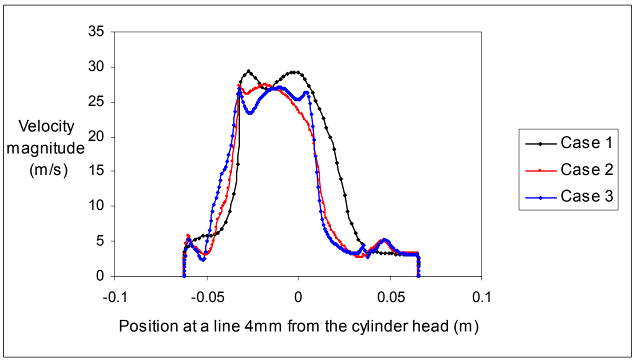

Fig. 4: Velocity magnitudes for different cases.

In order to improve and correctly represent the wall influence on boundary layer [14] the number of layers has been increased at least to fifteen layers.

5. MODELING VALIDATION

For validation purposes, intake airflow motion in an engine cylinder is simulated and the result is compared with the experimental data. Fig. 5 shows the simulation model of the engine cylinder [15]. Intake port connection is at the centre of cylinder and the intake valve lift is fixed to 7 mm. The simulation was done with the curvature of the intake port taken to be one (R/D=1).

The same grid generation is used here with a Mesh interval of 1mm and 1,112,000 cells. The boundary conditions are as follows: a uniform velocity distribution (mass flow rate of 25.4 g/s) at the intake port opening and atmospheric condition (101.3kPa, 293 K) at the bottom of the cylinder. Figs. 6 shows a comparison between the simulation results and the experimental result by Kawazoe et al. [16]. Fig. 7 shows the instantaneous velocity vector using numerical calculations. Many unsteady turbulence eddies are generated in the cylinder in spite of the steady boundary conditions.

The experimental result show flow circulation under the intake valve. Although the intake port is aligned to vertical axis, the airflow inducted to the cylinder is not symmetrical and circulation generation is weaker on one side. The CFD results confirm these phenomena as expected and shown experimentally.

For approaching the actual internal combustion engine unsteady flow CFD simulation, the behavior of different turbulence models has been evaluated by means of the analysis of a compressible turbulent flow in an engine cylinder encounters separation, recirculation and highly spatially varying shear stress. This test case, in fact, resembles the actual intake port connection with the engine head, allowing at the same time the analysis of separated flow, which is one of the most critical issues in turbulence simulation.

The velocity fluctuations and the turbulence characteristics of flow in this test case are more critical from the current problem (high turbulent I.C.E flow). So validating the model with this test case ensures the validity of the solution procedure.

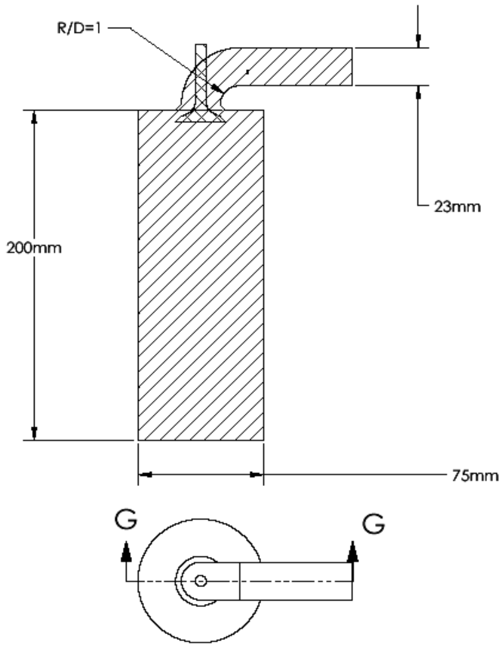

Fig. 5: Experimental test case is used for validation of the CFD results.

6. CALCULATION RESULTS

6.1 CYLINDER EVENTS DURING INTAKE AND COMPRESSION STROKES.

Early in the induction process, a set of conical jet of air impinges on the cylinder wall and piston that causes a strong interaction and a toroidal vortex appears in the periphery of cylinder (see Fig. 8). At the center, conical air jets collide and impinge on the bowl of combustion chamber, creating another toroidal vortex. During this phase, the turbulent velocity is further destabilized specially in the zones where re-circulation is maximum. In Fig. 9, the non-dimensional velocity field along a cross section at 10 mm from the cylinder head confirms that there are several vortices present with no predominant pattern. However, there is symmetry of the velocity flow field with respect to a vertical plane between the two intake valves.

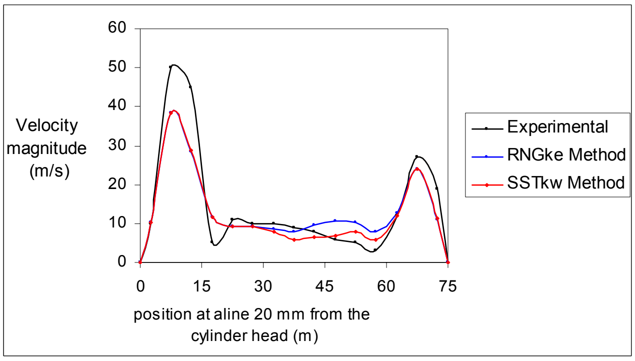

Fig. 6: Comparison of velocity magnitudes for three mesh cases.

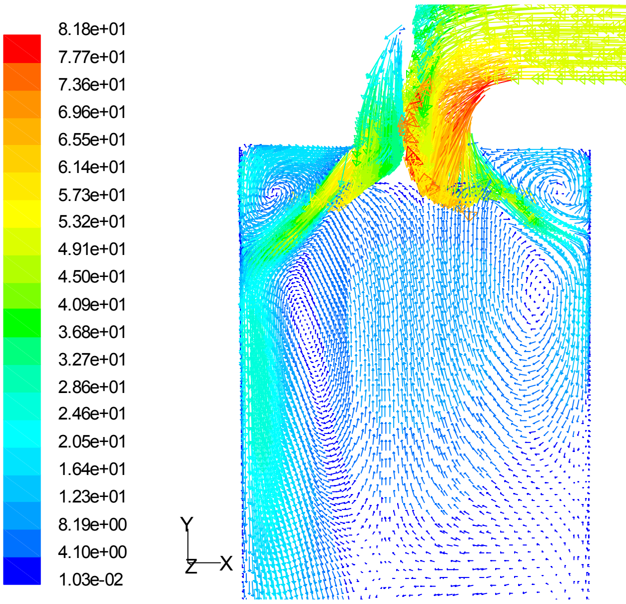

Fig. 7: Instantaneous velocity vectors at 40ms using RNG $\kappa\varepsilon$.

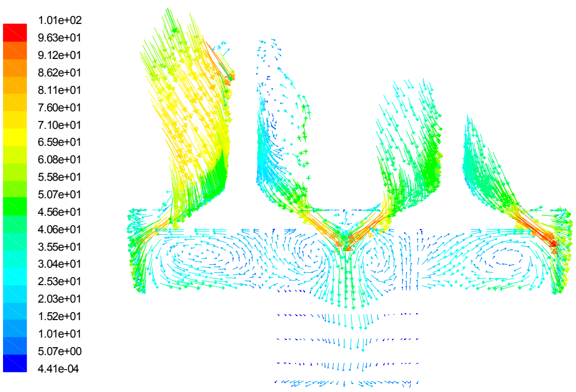

Fig. 8: Start of intake stroke: 40 degree crank angle on section CC.

As the intake stroke proceeds, the volume increases which leads to the development of a single vortex in the cylinder and shows the increased swirl in the downstream sections near the piston. In Fig. 10 the non-dimensional velocity field along a cross section passing through the axis of one of the valves and the axis of the cylinder is represented at 150 degrees after top dead center in the intake stroke.

At this stage, the piston speed is nearly constant and the intake valves are fully open. The toroidal vortex that was generated in the early stages of intake process has already disappeared. However, a new clockwise vortex is visible in the center of the cylinder because of the air jet motion towards the central part of the cylinder, which does not collide directly with the cylinder walls. The air jet impingement to the wall is deflected axially towards the piston surface and forms an elongated vortex along the wall Fig. 10.

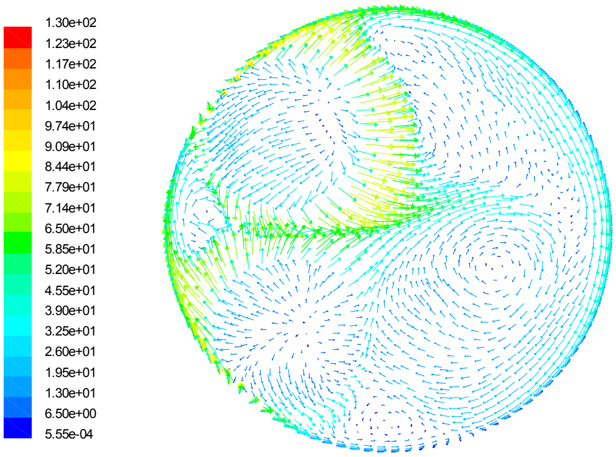

Fig. 9: Non-dimensional velocity field on a cross section at 10 mm from the cylinder head.

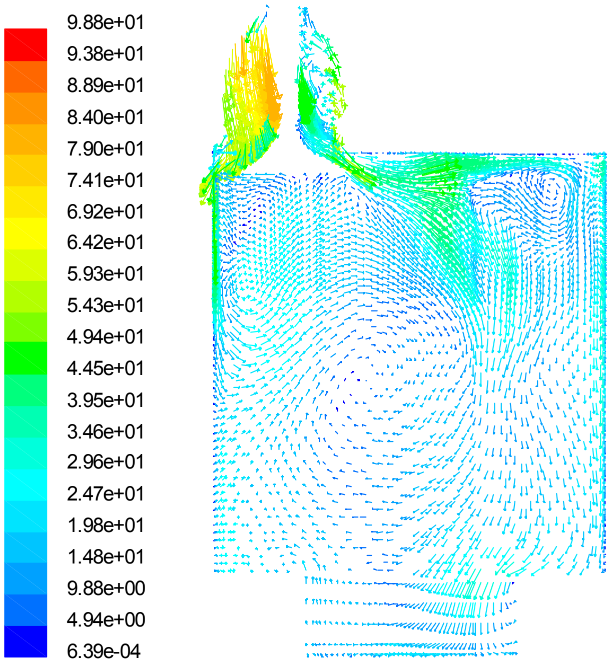

Fig. 10: Velocity field at 150 degree crank angle on section BB.

6.2 COMPARISON OF DIFFERENT TURBULENCE RESULTS

There is no significant difference for three turbulence models. In the case of piston bowl there is a strong interaction between squish and swirl near TDC. The centrifugal forces caused by the tangential vortex impede the flow from entering radially towards the central zone of the cylinder. Hence, in the three turbulence models considered, two toroidal vortices with opposite rotational directions appear in the combustion chamber at TDC (Fig. 11).

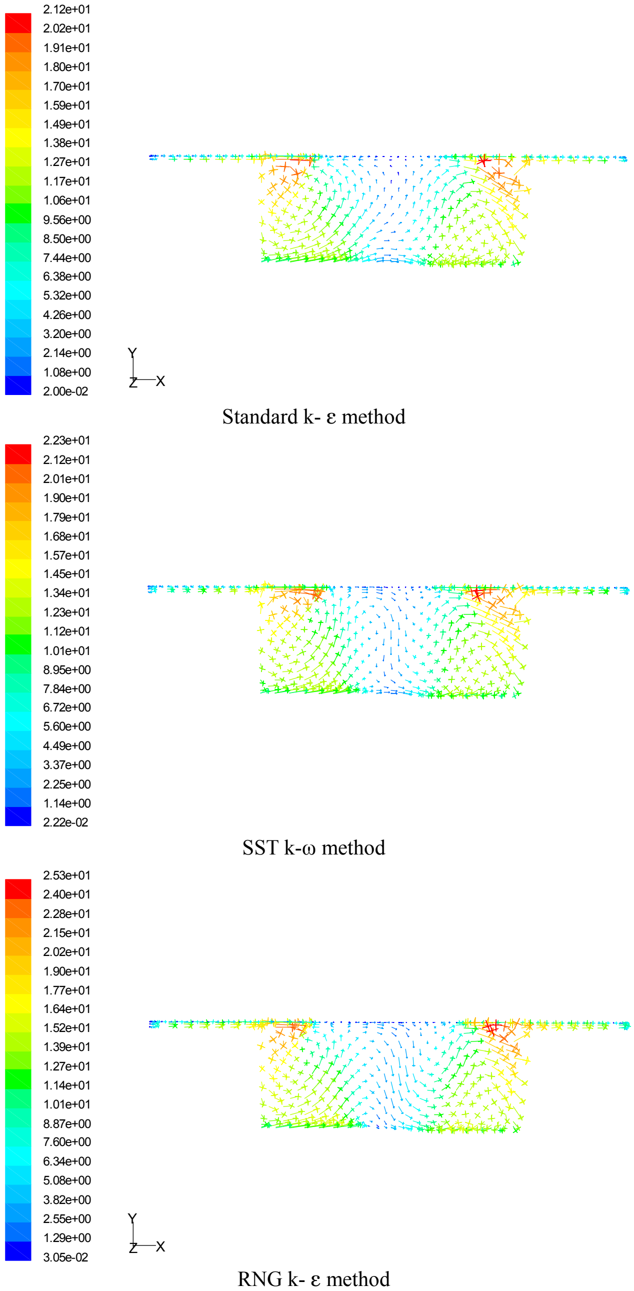

Fig. 11: Velocity vectors at TDC on section AA.

In the first model the flow field characteristics is symmetrical to some extent but vortices in the left hand are larger due to inlet valve positioning. In the second model the velocity flow field is not symmetrical and the vortices in the left hand are dominant. This can be explained due to valve positioning again. In the third model the velocity flow field is symmetrical and vortices in left and right are similar, this can be explained in terms of dying away of the turbulence intensity in the flow field. Analysis of Fig. 12 Indicates that the standard $\kappa-\varepsilon$ model generally returns the highest level of turbulence intensity. This is a typical defect of the Boussinesq stress-strain relation used in this model, which tends to return excessive levels of energy in presence of extensive strain. The RNG model returns the lowest levels of turbulence intensity confirming its characteristics under dissipative nature. $sst\kappa\omega$ and $RNG\kappa\varepsilon$ turbulence models yield almost same values for the turbulence intensity.

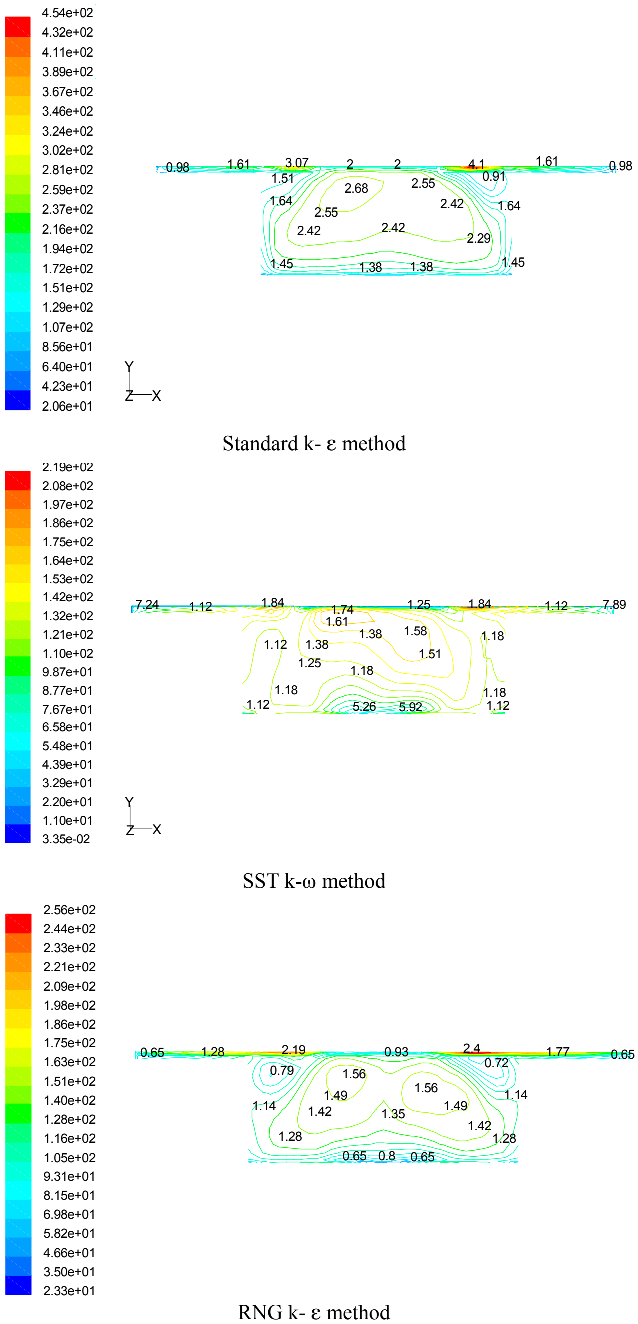

Fig. 12: Turbulent intensity contours at TDC for three-turbulence model on section AA.

7. CONCLUSION

In this paper, the performance of various turbulence models in simulation of unsteady three-dimensional high turbulence flow at intake and compression strokes have been evaluated.

The results show that there is no significant difference in the velocity flow field for different turbulence models. And also we can find out that using different turbulence models yields almost same values for the mass average pressure and swirl ratio and that the velocity flow field doesn't differ with $sst\kappa\omega$ and $RNG\kappa\varepsilon$ turbulence models. On the other hand, the turbulent velocity changes due to it dependence on the equations of the turbulence model used. For the parameters like pressure and swirl ratio the number of cells used is adequate.

$sst\kappa\omega$ and $RNG\kappa\varepsilon$ models yield almost the same results and seem suitable to simulate flow field parameters in the combustion chamber.

The application of different models on an engine cylinder steady flow indicated that standard $\kappa-\varepsilon$ model failed to simulate the case. In this case, $sst\kappa\omega$ model revealed to provide the most accurate results.

REFERENCES

[1] Heywood JB. "Fluid Motion Within the Cylinder of Internal Combustion Engines". The 1986 Freeman Scholar Lecture, J Fluids Eng 1986;109(1987):3–35.
[2] Kang KY, Reitz RD. "Intake Flow Structure and Swirl Generation in a Four-Valve Diesel Engine". Spring Technical Conference, ASME 1999, ICE-vol. 32-2. Paper No. 99-ICE-182, 1999.
[3] Yun J-E. "New Evaluation Indices for Bulk Motion of In-Cylinder Flow Trough Intake Port System in Cylinder Head". Proc IMechE, Part D: J Automobile Eng 2002;216:513–21.
[4] Desantes JM. Pastor JV. Doudou A. "Study of the Steady Flow Produced by Direct Injection Diesel Engine Intake Ports". Proc IMechE, Part D 2001;215:285–98.
[5] Fansler TD. "Turbulence Production and Relaxation in Bowl-In-Piston Engines", SAE Paper No.930479, 1993.
[6]. John B. Heywood. "Internal Combustion Engine Fundamentals". McGraw-Hill Book Company.
[7] G. Cantor, S.Fontanesi and E. Mattarelli. G. M. Bianchi. "A Methodology for In-Cylinder Flow Field Evaluation in a Low Stroke to Bore SI Engine", SAE Paper No. 2002-01-1119.
[8]. B. E. Launder and D. B. Spalding. "Mathematical models of turbulence", Academic Press, 1972.
[9]. B. E. Launder and D. B. Spalding. "The Numerical Computation of Turbulent Flows". Computer Methods in Applied Mechanics and Engineering, Vol. 3, 1974.
[10]. V. Yakhot, Smith, L. M., "The Renormalization Group. The $\varepsilon-$Expansion and Derivation of Turbulence Models" J. Science and Computer., Vol. 7, PP. 35-62, 1992.
[11] V. Yakhot, A. Orszag, S. THangam, T. B. Gataki, C. G. Speziale, "Development of Turbulence Models for Shear Flows by a Double Expansion Technique", Physics of Fluids A, Vol. 4, PP. 1510-1520, 1993.
[12]. D. C. Wilcox. Turbulence Modeling for CFD. DCW Industries, Inc., La Canada, California, 1998.
[13] B. Nkonga. "On the Conservative and Accurate CFD Approximations for Moving Meshes and Moving Boundaries". Comput. Methods Appl. Mech. Engrg. 190 (2000) 1801-1825.
[14] G. M. Bianchi. G. Cantore and S.Fontanesi. "Turbulence Modelling in CFD Simulation of ICE Intake Flows: The Discharge Coefficient Prediction", SAE Paper No. 2002-01-1118.
[15] Yoshihiro Sukegawa, Toshiharu Nogi, Yusuke Kihara. "In-Cylinder Air Flow of Automotive Engine by Quasi-Direct Numerical Simulation". JSAE Review 24 (2003) 123–126.
[16] Kawazoe etal ., Proc. 68th JSME Nat. Symp. C (500-9) (1990) (in Japanese).
[17] Witze PO. "Measurements of the Spatial Distribution and Engine Speed Dependence of Turbulent Air Motion in an ICEngine. SAE Paper No. 770220, 1977.
[18] F. Payri, J. Benajes, X. Margot, A. Gil. "CFD Modeling of the In-Cylinder Flow in Direct-Injection Diesel Engines". Computers & Fluids, 33-(2004) 995–1021.

NOMENCLATURE

V_p	Mean piston speed (m/s)
D	Diameter of the cylinder (m)
k	Turbulent kinetic energy (m2/s2)
n	Engine speed (rpm)
r	Radial coordinate (m)
SR	Swirl ratio (non-dimensional)
ν	Tangential velocity (m/s)
ε	Dissipation rate of turbulence (m2/s3)
ω	Dissipation rate of turbulence (m2/s3)
cad	Crank angle degree
TDC	Top dead center
BDC	Bottom dead center

APPENDIX A

The locations of cutting sections AA, BB and CC are given in this figure.